THE ASTROPHYSICAL JOURNAL, 218:461–467, 1977 December 1

INTERPRETATION OF BETA LYRAE. III. A STUDY OF THE DISK AROUND THE SECONDARY COMPONENT

DEBORAH A. BROWN AND SU-SHU HUANG
Department of Physics and Astronomy, Northwestern University
Received 1977 April 11; accepted 1977 May 26

ABSTRACT

We have analyzed light curves of β Lyrae available in the far-ultraviolet, visual, and infrared regions of the spectrum at numerous phases in eclipse in order to investigate the physical and radiative nature of the disk surrounding the secondary component. The results of our analysis together with those of other investigators lead us to propose that the outer regions of the disk are dominated by free electrons. This electron-scattering envelope is most likely the source of infrared radiation, as well as the cause of the observed polarization. However, the radiation in the region from the optical to the far-ultraviolet comes mainly from submerged layers where local thermodynamic equilibrium prevails. These layers represent the photosphere of either the disk or the secondary component itself.

Subject headings: stars: eclipsing binaries — stars: individual

I. INTRODUCTION

The idea that a disk surrounds the secondary component of β Lyrae (Huang 1963, hereafter Paper I) is now generally accepted and has been an integral part of many attempts to understand the observed properties of the system (Woolf 1965; Coyne 1970; Stothers and Lucy 1972; Kříž 1974; Wilson 1974; Hack *et al.* 1976). However, there is currently no general agreement on the physical nature of the disk itself. An analysis by Huang and Brown (1976*a*, hereafter Paper A; 1976*b*, hereafter Paper II) of the light curves of this system indicated that the disk showed characteristics of being in the state of LTE. This result seemed to discount the importance of electron scattering in the outer layers of the disk, a mechanism proposed by Huang (cf. Struve 1957) to explain the broadening of certain primary lines during eclipse and considered necessary in order to account for the observed periodic variation of polarization (Shakhovskoj 1964; Appenzeller and Hiltner 1967; Coyne 1970; McLean 1977). In this paper we will resolve this apparent contradiction between LTE and electron scattering by proposing a model based on a study of light curves that range from the far-ultraviolet to the infrared (Kondo, McCluskey, and Eaton 1976; Larsson-Leander 1969; Jameson and Longmore 1976).

II. AN ANALYSIS OF THE VISUAL, BLUE, AND FAR-ULTRAVIOLET LIGHT CURVES

In Paper A, we presented an elementary theory of the eclipsing depths of light curves and applied it to Beta Lyrae at phases 0.0 and 0.5. In this section we will extend the application to an arbitrary pair of phases θ, in primary eclipse, and $\pi + \theta$, half a period later in secondary eclipse. (The phase angle θ is measured from mid-primary eclipse.) Let $\Delta L_1(\theta, \lambda)$ be the radiation emitted at wavelength λ by the area of the primary eclipsed at θ and $\Delta L_2(\pi + \theta, \lambda)$ be the radiation emerging at λ from the surface area of the disk eclipsed at phase $\pi + \theta$. Then the ratio of the depth of the light curve at $\pi + \theta$ to that at θ, denoted by $(d_2/d_1)_{\lambda,\theta}$ where λ is the effective wavelength of the light curve, is

$$\left(\frac{d_2}{d_1}\right)_{\lambda,\theta} = \frac{\Delta L_2(\pi + \theta, \lambda)}{f_\theta \Delta L_1(\theta, \lambda)} . \quad (1)$$

The quantity f_θ, which may be called the shielding factor and is introduced here for the first time, is included to take care of the effects of the envelope around the secondary component, which may or may not completely block the radiation from the eclipsed area of the primary component at a given phase. It will be equal to 1 if the regions of the disk eclipsing the primary are opaque and the shielding is perfect. But if the eclipsing regions of the disk are semi-transparent, then f_θ will be less than 1. Roughly, $f_\theta = 1 - \exp(-\tau_\theta)$, where τ_θ is the average opacity of the disk along the line of sight averaged over the eclipsing area of the disk at θ. The depths in the light curve, d_1 and d_2, will be measured from a line through the flux levels at phases -0.25 and $+0.75$. This is the only line of reference that can be objectively drawn without assuming an exact model for the system. However, this means that implicit in equation (1) is the assumption that the total light emitted by the system in the direction of the observer (neglecting the effect of eclipses) is constant with phase. Thus what we will derive from equation (1) must be regarded as a zero-order approximation to the problem. At the end of this section, we will consider the departure of the shape of the primary component from spherical as a perturbation and examine the consequences of this perturbation.

In order to use equation (1) in practice, we may replace $\Delta L_2/(f_\theta \Delta L_1)$ by

$$\left(\frac{d_2}{d_1}\right)_{\lambda,\theta} = \frac{w_y F_2(T_y, \lambda)}{F_1(T_1, \lambda)}, \quad (2)$$

where $F_1(T_1, \lambda)$ is the flux of radiation from the eclipsed area of the primary component and T_1 is the average temperature of that eclipsed area. $F_2(T_y, \lambda)$ is the function giving the spectral distribution of the flux emerging from the eclipsed surface area of the disk. This flux might be due to any number of mechanisms or combinations of mechanisms. One possibility is thermal radiation from the embedded secondary component. Another is radiation from the disk itself. A third is radiation from shocks, resulting from mass flow. An understanding of the exact physical meaning of the temperature, T_y, that characterizes this flux, must therefore be postponed until the results obtained by using equation (2) are interpreted and the origin of the flux, F_2, is known. The correction factor w_y may be expressed by

$$w_y = \frac{D}{f_\theta}\left(\frac{\Delta A_2}{\Delta A_1}\right)_\theta, \quad (3)$$

where ΔA_1 is the projection of the surface area of the primary component eclipsed at θ onto the plane tangent to the celestial sphere, ΔA_2 is the projection of the area of the secondary component (and disk) eclipsed at $\pi + \theta$, and D includes other effects already discussed in Paper A. We shall assume w_y to be independent of wavelength in the following analysis, even though in reality it may not be so.

We will apply equation (2) to one visual and one blue light curve (Larsson-Leander 1969) and to five far-ultraviolet light curves (Kondo, McCluskey, and Eaton 1976). We are omitting Kondo *et al.*'s light curve at 1910 Å since that region is apparently distorted by Fe III emission (Hack *et al.* 1976). The reduced light curves of Kondo, McCluskey, and Eaton (1976) have more detail than their provisional light curves (Kondo, McCluskey, and Houck 1971) which were analyzed in Paper A at phases 0.0 and 0.5. And so, in this paper we will apply equation (2) to 21 pairs of phases, θ and $\pi + \theta$, in eclipse in addition to phases 0.0 and 0.5. For a given choice of θ and $\pi + \theta$, we measure d_1 (at θ) and d_2 (at $\pi + \theta$) from each available light curve. (The ratios of these depths are tabulated in Table 1 in the 5470, 4400, 3320, 2980, 2460, 1550 (tangent), and 1430 (tangent) columns. The meaning of the two remaining columns for the 1430 Å and 1550 Å regions will be discussed shortly.) For F_j ($j = 1, 2$) we will use Planck flux. For T_1, we adopt 11,350 K, which corresponds to a spectral type of B8.5 (Morton and Adams 1968). We then solve equation (2) for T_y at the effective wavelength of each light curve, after assuming some value of w_y. In this way we obtain as many values of T_y as there are light curves. From these values of T_y, we compute an average temperature, $\langle T_y \rangle$, and the root mean square (RMS) of the deviations of the individual temperatures from the average value. Thus for the assumed w_y we have derived values of $\langle T_y \rangle$ and RMS. By repeating the calculation for many choices of w_y, we will eventually find a minimum value of RMS. The pair of w_y and $\langle T_y \rangle$ corresponding to this minimum give the best fit of equation (2) to the data. This procedure may be followed for numerous pairs of phases θ and $\pi + \theta$ so that the run of $\langle T_y \rangle$ and w_y across the side of the disk facing the primary component is derived.

TABLE 1

MEASURED VALUES OF d_2/d_1 IN UNITS OF FLUX AS A FUNCTION OF WAVELENGTH AND PHASE

	λ (Å)								
$\pi + \theta$ (degrees)	1430 (tangent)	1430 (raised)	1550 (tangent)	1550 (raised)	2460	2980	3320	4400	5470
119.....	1.84	3.12	1.16	1.56	1.61	1.00	1.02	1.77	1.73
124.....	1.65	2.42	1.44	1.77	1.23	1.00	1.30	1.47	1.41
130.....	1.81	2.41	1.38	1.50	1.18	1.00	1.34	1.34	1.19
135.....	1.61	2.14	1.46	1.51	1.02	0.95	1.31	1.24	1.00
141.....	1.12	1.35	1.25	1.30	0.94	0.86	1.11	1.09	0.86
147.....	1.09	1.29	0.94	0.99	0.83	0.82	0.90	0.97	0.78
152.....	0.78	0.92	0.74	0.80	0.66	0.63	0.69	0.71	0.74
158.....	0.70	0.81	0.66	0.70	0.61	0.56	0.57	0.63	0.66
163.....	0.70	0.79	0.67	0.70	0.61	0.57	0.56	0.57	0.60
169.....	0.76	0.84	0.73	0.75	0.65	0.59	0.57	0.57	0.60
174.....	0.79	0.87	0.76	0.79	0.66	0.58	0.58	0.57	0.59
180.....	0.86	0.94	0.80	0.83	0.68	0.62	0.62	0.57	0.58
186.....	0.92	1.01	0.80	0.82	0.67	0.62	0.63	0.56	0.57
191.....	0.93	1.04	0.78	0.81	0.69	0.62	0.63	0.54	0.54
197.....	0.90	0.98	0.77	0.80	0.66	0.61	0.63	0.53	0.55
202.....	0.85	0.97	0.73	0.79	0.66	0.61	0.63	0.52	0.54
208.....	0.88	1.01	0.73	0.79	0.67	0.65	0.69	0.56	0.56
213.....	0.93	1.06	0.74	0.82	0.64	0.72	0.79	0.58	0.63
219.....	1.15	1.35	0.85	0.95	0.77	0.86	0.92	0.68	0.80
225.....	1.43	1.64	1.14	1.20	0.86	0.89	0.98	0.72	0.90
230.....	2.17	2.10	1.35	1.40	0.90	0.95	1.08	0.86	1.00
236.....	3.80	3.16	1.66	1.70	0.97	1.07	1.28	1.00	1.00

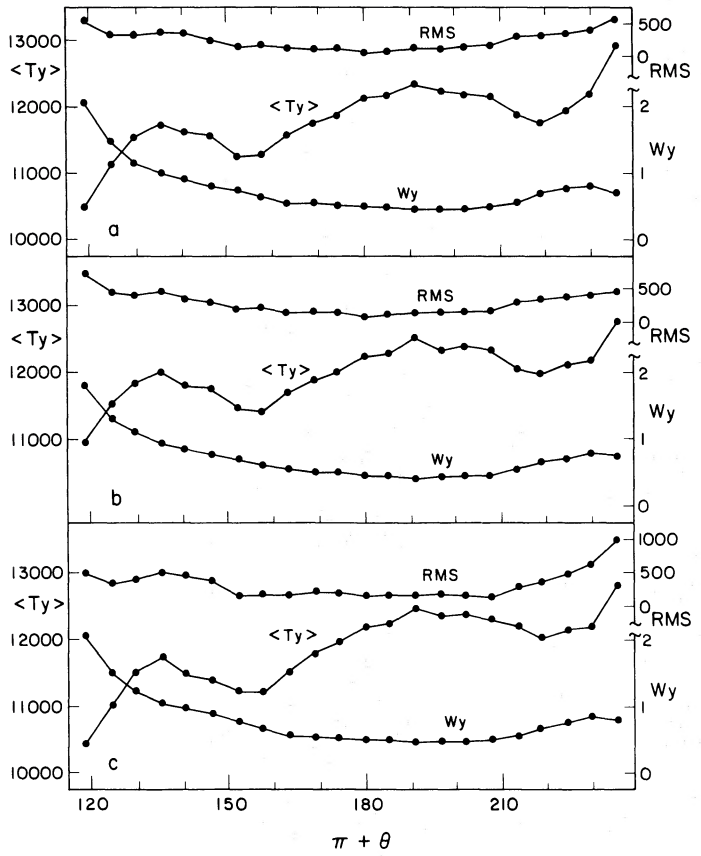

FIG. 1.—(*a*) From top to bottom, the RMS, $\langle T_y \rangle$, and w_y values corresponding to the most consistent fit of eq. (2) to the far-ultraviolet, blue, and visual light curves plotted against phase in secondary eclipse ($\pi + \theta$). Planck radiation was used for the flux. (*b*) The results of an analysis identical to that of Fig. 1*a* except that the depths used for the 1430 Å and 1550 Å light curves have been corrected for possible observational error. (*c*) The results of an analysis identical to that of Fig. 1*a* except that model atmosphere flux (Carbon and Gingerich 1969) was used in eq. (2) instead of Planck radiation.

The results are displayed in Figure 1*a* where, from top to bottom, the corresponding values of RMS, $\langle T_y \rangle$, and w_y are plotted against $\pi + \theta$.

There are a number of sources of error that might affect the results of Figure 1*a*. Observationally, the photometry in the far-ultraviolet has not been repeated; and one puzzling feature of the present ultraviolet light curves is that maximum light decreases from phase -0.25 to phase $+0.75$ by roughly 0.05 mag in the 1550 Å region and by nearly 0.15 mag in the 1430 Å region. If for the 1430 Å and 1550 Å light curves the line through the flux at quadratures from which we measured the eclipse depths is raised at phase 0.75 half of the way to the position where it would be horizontal through phase -0.25, and if the light curve depths are remeasured from this line, we obtain the ratios in Table 1 in the 1430 (raised) and 1550 (raised) columns. If the same analysis is then performed as for Figure 1*a* but with the new depth ratios for the 1430 and 1550 Å regions, we obtain Figure 1*b*. These curves show the same general behavior as those of Figure 1*a*.

The use of Planck radiation for the F_j ($j = 1, 2$) in equation (2) is only for rough purposes. Nonetheless, when an analysis is done with model atmosphere flux (Carbon and Gingerich 1969), the results are very much like those of Figure 1*a*. They are presented in Figure 1*c*. For these results we used the same eclipse depth ratios as for Figure 1*a*. Just as for Figures 1*a* and 1*b*, we did not correct for the presence of emission lines observed at wavelengths less than 2200 Å (Hack *et al.* 1976) since Hack *et al.*'s (1977) results indicate that the depth ratios of the 1430 Å and 1550 Å light curves cannot be explained by emission.

As discussed earlier, equation (1) is an approximation for the eclipse depth ratios measured from the light at quadrature since it neglects the change with phase of the total light emitted by the system in the direction of the observer. Actually, we know that the primary is tidally distorted, i.e., elongated along the common axis of the two components. If we consider the departure of the shape of the primary component from a sphere as a perturbation, this perturbation is symmetric with respect to the line joining the two components. It follows that the results of this perturbation on T_y and w_y should be symmetric in sign with respect to $\pi + \theta = 180°$. Hence the perturbation will not alter the increasing trend of $\langle T_y \rangle$ in Figure 1.

For the same reason, if the temperature variation around the circumference of the primary component is symmetric with respect to the common axis (Alduseva 1973), it would not change the trend of $\langle T_y \rangle$ with $\pi + \theta$. However, if the temperature variation over the surface has no definite pattern, the problem becomes too involved to be treated here.

The symmetric perturbation may enhance or it may dampen the curvature of the w_y and RMS curves. We have calculated a trial case that attempts to allow for the distorted primary component by arbitrarily introducing a level of maximum flux that decreases smoothly from the quadratures toward mid-eclipse. While the eclipse depth ratios found from this level indeed change, the features of the curves in Figure 1 are not only preserved but they are enhanced.

III. THE SOURCE OF THE INFRARED RADIATION

Jameson and Longmore (1976) have published five infrared light curves of β Lyrae in the range 1.25–8.6 μm. These show that secondary eclipse becomes deeper than primary eclipse for wavelengths longer than 3.5 μm. We will analyze four of their light curves at mid-eclipse to investigate this behavior, omitting their 8.6 μm light curve because of its lack of symmetry. The central eclipse depth ratios, measured from the quadratures, are tabulated for these four light curves in Table 2. When equation (2) is applied to the far-ultraviolet, blue, visual, and infrared light curves at mid-eclipse, using Planck flux for F_1 and F_2, the best fit to the flux emerging from the disk occurs for $\langle T_y \rangle = 9490$ K, $w_y = 1.25$, and RMS = 1140 K. Such a high RMS value indicates that the flux emerging from the disk must consist of light from at least two sources, since application of equation (2) to only the ultraviolet, blue, and visual light curves yielded an RMS value on the order of 100 K for blackbody radiation in Figure 1. The second source evidently radiates significantly only in the infrared. We can investigate the nature of this second source by analyzing the eleven light curves at phase 0.0 using an equation with two components for the radiation emerging from the disk, namely,

$$\left(\frac{d_2}{d_1}\right)_{\lambda,0} = \frac{w_y F_2(T_y, \lambda) + w_z F_2'(T_z, \lambda)}{F_1(T_1, \lambda)} . \qquad (4)$$

For F_1, F_2, and F_2', let us use Planck radiation. For the first component of radiation from the secondary, $w_y F_2(T_y, \lambda)$, we may use $w_y = 0.45$ and $T_y = 12{,}000$ K, the approximate values in Figure 1*a* for the flux emerging from the disk in the 1430–5470 Å range. We may also let $T_1 = 11{,}350$ K. Then for a given value of w_z we may solve equation (4) for T_z, the temperature of the infrared component of radiation from the disk, at the effective wavelengths of each of the 11 light curves. Performing the same sort of analysis as for equation (2), we find that the best fit to the light curves occurs for $\langle T_z \rangle = 6310$ K, $w_z = 1.2$, and RMS = 1710 K. Apparently this excessively large value of RMS means that the infrared component of radiation, F_2', is from a source that radiates quite differently from a blackbody. Thus we have shown what has been suspected by Jameson and Longmore (1976) and Hack *et al.* (1977), namely, that it is nonthermal in origin.

It is evident from polarization studies of β Lyrae (Coyne 1970; Appenzeller and Hiltner 1967) that free electrons are present in large numbers in the outer layers of the disk. And so one possible mechanism for the excess infrared radiation is free-free emission, similar to that observed from the envelopes of Be stars (Woolf, Stein, and Strittmatter 1970; Gehrz, Hackwell, and Jones 1974). Let us see if the spectral distribution of the infrared component is consistent with that of free-free emission. From equation (4), the spectral distribution of the total flux from the secondary component and disk at phase 0.0 is given by

$$F_0(\lambda) = \left(\frac{d_2}{d_1}\right)_{\lambda,0} F_1(T_1, \lambda) . \qquad (5)$$

Let us take $T_1 = 11{,}350$ K and Planck flux for F_1. Then the values of $F_0(\lambda)$ calculated from equation (5) are plotted in Figure 2 as open circles. Next we assume that $F_0(\lambda)$ consists of two components of radiation, just as in equation (4). The first of these, $w_y F_2(T_y, \lambda)$, is the thermal source found in Figure 1*a*. Taking values of $w_y = 0.48$ and $T_y = 12{,}000$ K, close to those of Figure 1*a*, and using Planck radiation for F_2, we

TABLE 2

MEASURED VALUES OF d_2/d_1 IN THE INFRARED AT PHASE 0.0

$\lambda(\mu m)$.....	1.25	2.2	3.6	4.8
d_2/d_1.....	0.54	0.76	1.12	1.10

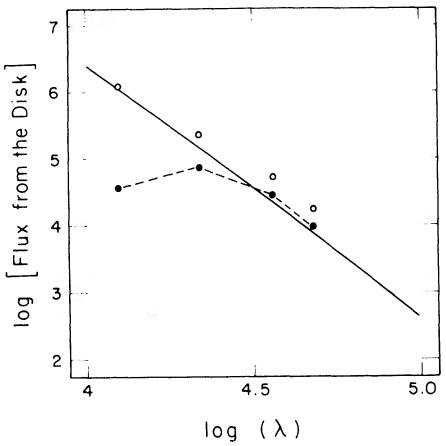

FIG. 2.—*Open circles*, the spectral distribution of the total flux from the disk calculated from eq. (5). *Solid line*, the distribution of the thermal flux due to the 12,000 K ($w_y = 0.48$) component of radiation found from an analysis of the ultraviolet, blue, and visual light curves. The distribution of the excess infrared radiation found by subtracting the flux due to the 12,000 K component from the total flux is plotted as the filled circles and connected by the dashed curve.

may calculate the distribution of this flux in the infrared. It is plotted in Figure 2 as the solid line. The distribution of the flux due to the second component of radiation, the one that radiates primarily in the infrared (F_2'), may be calculated by subtracting $w_y F_2(T_y, \lambda)$ from $F_0(\lambda)$. This difference is plotted in Figure 2 as the filled circles and is connected by the broken line, the trend of which appears to be consistent with emission due to free-free transitions.

IV. A MODEL FOR THE DISK

In this section, we will propose a model for the disk that incorporates the condition of local thermodynamic equilibrium (LTE) found in Paper A, the electron scattering layer detected by the polarimetry (Appenzeller and Hiltner 1967; Coyne 1970), and the observed infrared excess (Jameson and Longmore 1976). We will then show that the results of Figure 1 are qualitatively consistent with our model. For purposes of illustration, we may visualize the system roughly as it is presented in Figure 3 in the plane of the orbit. The primary component is depicted in solid black, and the upper layers of the disk are crosshatched. The mottled black condensation inside the disk will be discussed shortly. Also pictured is the gas stream from the primary to the disk (Struve 1941). The dimensions are based on those derived by Wilson (1974) from the visual and blue light curves for a mass ratio of 4 and are used only for purposes of illustration. The relative sizes and shapes are not meant to be taken literally.

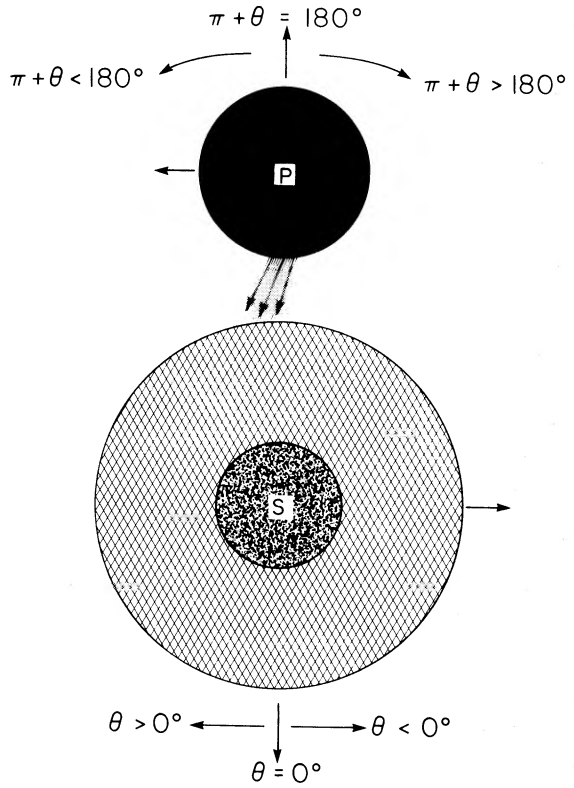

FIG. 3.—Schematic picture of system in the plane of the orbit. The relative dimensions and shapes of the components used are for purposes of illustration only and have not been derived here.

Let us now consider the physical nature of the disk. The outer layers of the disk are rarefied and hot enough to be highly ionized and semitransparent to light in the far-ultraviolet and visual regions. One source of the energy for ionization is most likely provided by shock waves set up in the system as a result of mass flow. In any case the main source of opacity for these outer layers in the far-ultraviolet and visual regions is electron scattering. Beneath the outer layers are intermediate layers where the temperature, density, and degree of ionization may vary. At some depth beneath the surface, the gas becomes dense enough to radiate light under conditions of LTE. This layer or "photosphere" of the disk, which is presented schematically in Figure 3 in mottled black, could be either the surface of the embedded secondary star or some level of the disk itself. In addition to the scattered light, the intermediate and upper layers of the disk radiate some light of their own. This light is largely subordinate to the flux from the submerged photosphere in the region from the optical to the far-ultraviolet, but becomes dominant in the infrared due to free-free processes.

Let us discuss the qualitative features of Figure 1 in terms of our model. In Figure 4 we present the projected areas of the components for six phases, θ, in primary eclipse and the six corresponding phases, $\pi + \theta$, in secondary eclipse. We have used the same relative dimensions for the components as those in Figure 3.

The general increasing trend of $\langle T_y \rangle$ with $\pi + \theta$ in Figure 1 has been shown to be real despite the approximate nature of equation (1). This trend can be easily explained as due to heating of the disk by the gas stream from the primary. From Figures 3 and 4 it is easy to see that this would result in more flux being emitted by the portions of the disk eclipsed after secondary minimum ($\pi + \theta > 180°$) than those eclipsed before secondary minimum ($\pi + \theta < 180°$), since the stream is deflected into the former region by the Coriolis effect.

Even though the RMS and w_y curves in Figure 1 are derived from a zero-order treatment of the eclipse depth ratios, they are consistent with our physical model. For example consider first phases near to and including mid-eclipse (Fig. 4, case 3). Near phase 0.0, the primary component is eclipsed mostly by the opaque central condensation of the disk and only partly by the more rarefied upper layers. Consequently, the shielding factor f_θ will be close to 1 in equation (3). We may also safely assume $(\Delta A_2/\Delta A_1) = 1$ since the orbit of β Lyrae is nearly circular (Struve 1958; Batten and Fletcher 1975). Then the value of $w_y < 1$ in Figure 1 must be due to some factor other than f_θ and $(\Delta A_2/\Delta A_1)$ in equation (3). We suggest that it is due to attenuation of the flux from the submerged photosphere (of the disk or the secondary component) during its passage outward through upper layers of

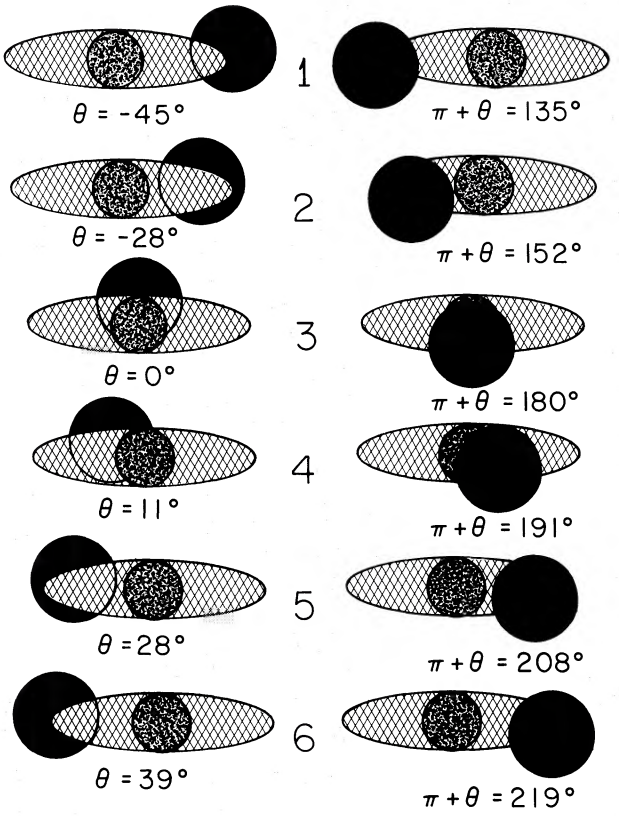

FIG. 4.—Schematic diagrams of the projected areas of the components onto the celestial sphere for six phases in primary eclipse and six corresponding phases in secondary eclipse. The dimensions and shapes of the components used are for purposes of illustration only.

the disk. The low values of RMS mean that the spectral distribution of the flux emerging from the eclipsed area of the disk is very nearly Planckian. This is consistent with the idea that electron scattering is a major source of opacity in the upper layers of the disk, since electron scattering is independent of wavelength. The low values of RMS also appear to indicate that the part of the emergent flux originating in the submerged photosphere is more important than the part originating in the upper layers under conditions deviating from LTE, since the latter part will not have a Planckian distribution.

In Paper A we were unable to find a component of light from the primary star reflected by the disk at phase 0.0. Perhaps some of the radiation from the primary is absorbed in the lower layers of the disk. Even though some of it would be scattered by free electrons in the upper layers of the disk, the fraction of this light scattered back toward the primary component would be insignificant compared to the radiation from the submerged photosphere.

The steady increase of the RMS curve with phase away from mid-eclipse, if real, indicates that the radiation emerging from the obscured part of the disk departs steadily from a blackbody distribution at a single temperature. From Figure 4, it is clear that as phase increases or decreases from mid-secondary eclipse, the primary component obscures increasingly the intermediate and upper layers of the disk and decreasingly the submerged photosphere. As this happens, the angle of emergence of the flux from the obscured portion of the disk changes, and an increasingly larger portion of this flux comes from the intermediate and upper layers of the disk as opposed to the submerged photosphere. Since physical conditions in these outer layers deviate from LTE, the flux emitted by them deviates from blackbody flux, thus causing the rise in the RMS values in Figure 1, where we tried to fit F_2 by Planck radiation.

Consider next the increasing trend of the w_y curves in Figure 1. From the configurations on the left in Figure 4, we see that as phase increases or decreases from mid-primary eclipse, the portion of the secondary component and disk eclipsing the primary component shifts from the opaque central condensation to more and more rarefied outer layers. These layers are less and less effective in obscuring the light radiated from the eclipsed area of the primary. As a result, the shielding factor f_θ will decrease. Then since $w_y \propto 1/f_\theta$, w_y will increase as θ either increases or decreases from 0°.

However, the increase in the w_y curve is asymmetric. This asymmetry, if real, might be due to the effects of the stream from the primary component, shown schematically in Figure 3. When the system is viewed at phases after mid-primary eclipse ($\theta > 0°$), the presence of the stream adds to the opacity of the disk to the light from the primary component. In addition, it is possible that the density of the disk is greater in its trailing hemisphere, where it is fed by the stream from the primary component, than in its leading hemisphere. Either one of these effects would result in a larger shielding factor, f_θ, for $\theta > 0°$ than for $\theta < 0°$. Then, by equation (3), w_y would be smaller for $\pi + \theta > 180°$ than $\pi + \theta < 180°$. Such an increased opacity due to the stream has already been postulated in Paper I to explain the asymmetry of primary eclipse found in the visual light curve and by Coyne (1970) to explain the nature of the maximum in the polarization curve found during primary eclipse.

So we see that the variations of w_y and RMS with phase derived from the zero-order approximation agree with what would be expected from the disk model for the system, which has been derived independently of these considerations in Paper I and is supported by other investigations (Woolf 1965; Appenzeller and Hiltner 1967; Coyne 1970; Wilson 1974). Therefore this agreement may indicate that the zero-order approximation provides us with reasonable results.

On the basis of our model, we might expect to see changes in the slope of the light curves during secondary eclipse when the primary component starts and ceases to eclipse the bright photosphere submerged in the disk. The 1430 Å, 1550 Å, and 1910 Å light curves (Kondo, McCluskey, and Eaton 1976) show a

standstill and shift to steeper slope at about JD = 2,440,898.2 ($\pi + \theta \approx 150°$) on the descending branch of secondary eclipse and a second standstill and change of slope, this time from steep to shallow, on the ascending branch at JD $\approx$ 2,440,900.8 ($\pi + \theta \approx 220°$) which may be the result of this discontinuity. Interestingly the changes in the slope become less noticeable with increasing wavelength for the 2460 Å, 2980 Å, and 3320 Å light curves but are again apparent to a small degree in the blue light curve (Larsson-Leander 1969). This might mean that the upper layers of the disk become less transparent at longer wavelengths in the far-ultraviolet and that their own radiation becomes increasingly more important with respect to the radiation from the submerged photosphere and impacting gas stream due to atomic processes in the disk, such as Balmer continuum absorption, even though on the average they are semitransparent in the 1430–5470 Å range. Whether this interpretation is significant or not remains to be investigated. However, the change in shape of the light curves with wavelength, if verified by future observations, is most likely due to a change in the optical properties of the disk with wavelength, just as Huang (1973) has suggested generally for most eclipsing binaries with envelopes.

The present investigation has been supported by a grant from the National Aeronautics and Space Administration.

REFERENCES

Alduseva, V. Ya. 1973, *Soviet Astr.—AJ*, **17**, No. 5, 619.
Appenzeller, I., and Hiltner, W. A. 1967, *Ap. J.*, **149**, 353.
Batten, A. H., and Fletcher, J. M. 1975, *Pub. A.S.P.*, **87**, 237.
Carbon, D. F., and Gingerich, O. 1969, in *Theory and Observation of Normal Stellar Atmospheres*, ed. O. Gingerich (Cambridge: MIT Press), p. 377.
Coyne, G. V. 1970, *Ap. J.*, **161**, 1011.
Gehrz, R. D., Hackwell, J. A., and Jones, T. W. 1974, *Ap. J.*, **191**, 675.
Hack, M., Hutchings, J. B., Kondo, Y., and McCluskey, G. E. 1977, preprint.
Hack, M., van den Heuvel, E. P. J., Hoekstra, R., de Jager, D., and Sahade, J. 1976, *Astr. Ap.*, **50**, 335.
Huang, S.-S. 1963, *Ap. J.*, **138**, 342 (Paper I).
———. 1973, *Ap. Space Sci.*, **21**, 263.
Huang, S.-S., and Brown, D. A. 1976*a*, *Ap. J.*, **204**, 151 (Paper A).
———. 1976*b*, *Ap. J.*, **208**, 780 (Paper II).
Jameson, R. F., and Longmore, A. F. 1976, *M.N.R.A.S.*, **174**, 217.
Kondo, Y., McCluskey, G. E., and Eaton, J. A. 1976, *Ap. Space Sci.*, **41**, 121.
Kondo, Y., McCluskey, G. E., and Houck, T. E. 1971, *IAU Colloquium No. 15*, p. 308.
Kříž, S. 1974, *Bull. Astr. Soc. Czechoslovakia*, **25**, 6.
Larsson-Leander, G. 1969, *Ark. Astr.*, **5**, 253.
McLean, I. S. 1977, *Astr. Ap.*, **55**, 347.
Morton, D. C., and Adams, T. F. 1968, *Ap. J.*, **151**, 611.
Shakhovskoj, N. M. 1964, *Astr. Zh.*, **41**, 1042.
Stothers, R., and Lucy, L. B. 1972, *Nature*, **236**, 218.
Struve, O. 1941, *Ap. J.*, **93**, 92.
———. 1957, in *Nonstable Stars*, ed. G. H. Herbig (Cambridge: Cambridge University Press), p. 93.
———. 1958, *Pub. A.S.P.*, **70**, 5.
Wilson, R. E. 1974, *Ap. J.*, **189**, 319.
Woolf, N. J. 1965, *Ap. J.*, **141**, 155.
Woolf, N. J., Stein, W. A., and Strittmatter, P. A. 1970, *Astr. Ap.*, **9**, 252.

DEBORAH A. BROWN and SU-SHU HUANG: Dearborn Observatory, Northwestern University, Evanston, IL 60201